

Passivity assessment and enforcement utilizing eigenpairs information

Bjørn Gustavsen

SINTEF Energy Research, P.O. Box 4761 Sluppen, NO-7465 Trondheim, Norway

ARTICLE INFO

Index Terms:

Passivity assessment
Passivity enforcement
Residue perturbation
Eigenpairs
Non-negative least squares

ABSTRACT

Rational models can be a cause of unstable time domain simulations if they are non-passive. One commonly applied method for ensuring model passivity is to combine a passivity assessment step with a passivity enforcement step in an iterative loop where the model's residue matrices are updated in each pass. This paper shows a new variant of such scheme that is computationally more efficient than an existing one. The advantage is achieved by transferring eigenpairs information between the two steps, rather than frequency samples where passivity violations exist. This leads to fewer inactive constraints in the constrained least squares problem associated with the passivity enforcement step, and thereby faster solving. The new approach is combined with the residue perturbation method known as RP-NNLS for maximum performance. The resulting procedure is demonstrated for the modeling of components with many terminals, a white-box transformer impedance matrix, grounding mat admittance matrix, and a black-box transformer model obtained via frequency sweep measurements.

1. Introduction

RATIONAL modeling techniques are essential tools in the modeling of power system components and subsystems for use in electromagnetic transient simulation studies. Typical examples include frequency-dependent modeling of transmission line/cable characteristics [1,2], frequency-dependent network equivalents [3,4,5,6] and transformer black-box modeling from measurements [7,8]. Very efficient modeling techniques are available [9,10,11] that can extract models from frequency samples, typically in the form of a pole-residue model or a state-space model. The models are constrained to satisfy the physical requirements of causality and stable poles [12], however the passivity condition must with most methods be enforced by a postprocessing step. The passivity property is essential since it is a fundamental requirement to guarantee stable behavior of a model when included in a time domain simulation environment.

Several passivity enforcement schemes have been proposed, e.g. perturbation of residue matrices [13] or their eigenvalues [14], or (equivalently) the state-space output matrix [15,16,17,18]. The perturbation is calculated in such way that the passivity condition is satisfied at frequencies where passivity violations are detected. These methods require iterations since a first order linearization is made when relating the passivity condition to the model design parameters. The iteration involves the solving of a passivity assessment step followed a passivity enforcement step. The passivity assessment can either be based

on the eigenvalues of the admittance matrix real part [19], or on the eigenvalues of a test matrix that relates the model's design parameters with the passivity condition [15,20]. In addition, passivity enforcement schemes have been proposed that do not require linearization [21,22]. These latter schemes, which are based on linear matrix inequalities (LMI), are usually too computationally demanding except for small-scale problems [17]. A detailed description of alternative passivity conditions and enforcement schemes is given in [23].

One of the iterative passivity enforcement schemes is residue perturbation (RP) [13]. Recently, one new variant [24] was proposed that converts the constrained least squares (LS) problem into a non-negative LS problem via QR factorization. The resulting method (RP-NNLS) was demonstrated to be highly efficient in solving problems with many terminals in terms of computation speed and memory usage. It was however pointed out [24] that the efficiency deteriorates when the NNLS problem to be solved includes many non-active constraints as the applied active set type solver will then require many iterations. The problem of inactive constraints becomes a major issue when combining RP-NNLS with the existing iterative scheme used in previous works [14, 25] since the information about passivity violations passed to the passivity enforcement step is in the form of frequency samples. As will be shown, such approach can lead to an excessive number of passivity constraints.

This paper proposes a new iterative scheme for use with RP methods that seeks to minimize the number of inactive constraints that can arise.

E-mail address: bjorn.gustavsen@sintef.no.

<https://doi.org/10.1016/j.epsr.2021.107041>

Received 29 September 2020; Received in revised form 23 December 2020; Accepted 14 January 2021

Available online 31 January 2021

0378-7796/© 2021 The Author. Published by Elsevier B.V. This is an open access article under the CC BY license (<http://creativecommons.org/licenses/by/4.0/>).

This is achieved by passing violating eigenpairs from the passivity assessment routine to the passivity enforcement routine, rather than frequency samples. It is shown that the number of constraints can then be strongly reduced in the case of models having many terminals. This alternative iterative scheme is combined with the RP-NNLS method to reach a highly efficient method. The resulting approach is demonstrated for three examples: Transformer branch impedance modeling (213 terminals, 10th order), ground mat admittance modeling (121 terminals, 30th order), and transformer measurement-based modeling (5 terminals, 90th order).

2. Problem statement

It is assumed a rational model on pole-residue form (1) with n terminals (ports). The model has stable poles a_i but it is not necessarily passive. The poles a_i and residue matrices \mathbf{R}_i are real or complex conjugate, and the model's admittance matrix \mathbf{Y} is symmetrical.

$$\mathbf{Y}^{n \times n}(\omega) = \mathbf{R}_0^{n \times n} + \sum_{i=1}^N \frac{\mathbf{R}_i^{n \times n}}{j\omega - a_i} \quad (1)$$

Passivity of the model is to be enforced by an iterative procedure where the model's passivity characteristics are assessed, followed by a passivity enforcement step which calculates a perturbation $\Delta \mathbf{R}_i$ to the residue matrices. It will be assumed that $\Delta \mathbf{R}_i$ is calculated using RP-NNLS by the active set method outlined in [24].

The objective is to introduce a new iterative passivity/assessment scheme such that the number of passivity constraints in RP-NNLS is kept as small as possible, thereby maintaining a high computational efficiency with RP-NNLS.

3. Samples method

The approach to be improved is the iterative scheme introduced in [25]. That approach has been applied in several works, e.g. in the "Matrix Fitting Toolbox" that is downloadable from the internet (<https://www.sintef.no/projectweb/vectfit/>). The information about passivity violations being passed from the passivity assessment step to the passivity enforcements step is in the form of two arrays of frequency samples, $\mathbf{s}2$ and $\mathbf{s}3$. As will be shown in Section 4 this samples-based information transfer will necessarily lead to an unnecessary high number of passivity constraints in the subsequent passivity enforcement step.

3.1. Passivity assessment step

Passivity entails that the model's (terminal) admittance matrix \mathbf{G} has positive eigenvalues at all frequencies [19],

$$\mathbf{G}(\omega) = \text{Re}\{\mathbf{Y}(\omega)\} > 0 \quad \forall \omega \quad (2)$$

Crossover frequencies are identified where eigenvalues of \mathbf{G} change sign. This can be done in two alternative ways:

- 1 Via the eigenvalues of the so-called half-size test matrix \mathbf{S} in (3) [20], or via the Hamiltonian (full-size) test matrix [15].
- 2 By calculating a frequency sweep of the eigenvalues of \mathbf{G} .

$$\mathbf{S} = \mathbf{A}(\mathbf{B}\mathbf{D}^{-1}\mathbf{C} - \mathbf{A}) \quad (3)$$

In the case of alternative 1 with \mathbf{S} , the square-root of any positive real eigenvalue of \mathbf{S} defines a crossover frequency where an eigenvalue of \mathbf{G} changes sign. The CPU time of the eigenvalue computation can however become excessive for large models and one must then instead use alternative 2.

By calculating the eigenvalues of \mathbf{G} at any frequency point between two successive crossover frequencies, bands of passivity violations are

established, see Fig. 1. In each violating band, the eigenvalues of \mathbf{G} are calculated as discrete, smooth functions of frequency where so-called artificial eigenvector switchovers are removed by a switching-back procedure. Details of this procedure is described in Section 5.4. In each violating band, the frequency associated with the maximum violation of each violating eigenvalue is stored in an array $\mathbf{s}2$. Fig. 1 shows an example of a passivity band where two eigenvalues are negative.

3.2. Passivity enforcement step

Passivity is enforced at frequencies given in $\mathbf{s}2$ by a residue perturbation (RP) method, in this case RP-NNLS. The enforcement seeks to calculate a minimum perturbation (4a) of the model such that all violations defined at frequencies $\mathbf{s}2$ are removed (4b). The samples used in (4a) are normally taken as those used when calculating the original model, e.g. by VF.

$$\Delta \mathbf{Y}(\omega) = \Delta \mathbf{R}_0 + \sum_{i=1}^N \frac{\Delta \mathbf{R}_i}{j\omega - a_i} \approx \mathbf{0} \quad (4a)$$

$$\mathbf{G}(\omega) + \Delta \mathbf{G}(\omega) = (\mathbf{R}_0 + \Delta \mathbf{R}_0) + \sum_{i=1}^N \frac{(\mathbf{R}_i + \Delta \mathbf{R}_i)}{j\omega - a_i} > 0 \quad (4b)$$

Eqs. (4a) and (4b) are solved simultaneously as a constrained linear least squares problem (5), where \mathbf{A} is established from (4a) and \mathbf{C} is established from (4b).

$$\min_{\mathbf{x}} \|\mathbf{A}\mathbf{x}\| \quad \text{s.t.} \quad \mathbf{C}\mathbf{x} > \mathbf{d} \quad (5)$$

The calculation of the constraint part of (5) is based on first order linear approximation between a matrix perturbation and the change to its eigenvalues [13,28]. This matrix perturbation is given by (6) when considering that \mathbf{G} is real and symmetrical and it has been assumed that the eigenvectors have been scaled to unit length [13]. $\Delta \mathbf{G}$ is the perturbed matrix, \mathbf{t}_j is a (right) eigenvector of \mathbf{G} , and $\Delta \lambda_j$ is the change to the associated eigenvalue.

$$\Delta \lambda_j \approx \mathbf{t}_j^T (\Delta \mathbf{G}) \mathbf{t}_j, \quad j = 1, \dots, n \quad (6)$$

3.3. Iterations

Since the constraint equation in (5) makes use of the linear approximation (6), the solving of (5) will not make a violating eigenvalue exactly zero at the prescribed frequency. Also, new violations may occur at other frequencies. Iterations are therefore needed where the process of assessment and enforcement is repeated until all eigenvalues are non-negative.

The robustness of the procedure is enhanced by complementing this (outer-loop) iteration with an inner-loop iteration which adds additional frequencies in an array $\mathbf{s}3$ if the passivity violations in $\mathbf{s}2$ results in

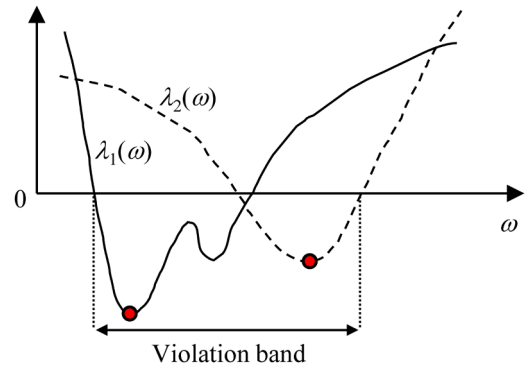


Fig. 1. Frequency band with passivity violations.

passivity violations at new frequencies. The program then steps back and uses the previous model while adding extra constraints at the frequencies in $\mathbf{s3}$. The impact of frequencies in $\mathbf{s2}$ and $\mathbf{s3}$ on the passivity enforcement is illustrated in Fig. 2. The left plot shows one violating eigenvalue associated with $\mathbf{s2}$ while the right plot shows one eigenvalue associated with $\mathbf{s3}$. The permitted range of the perturbed eigenvalue is indicated by the vertical arrow.

The total procedure is shown in Fig. 3. It is observed that the model is not updated during the inner-loop iterations, i.e. the same model (with residue matrices $\{\mathbf{R}_i\}_0$) is re-used but with more constraints. That way, extra constraints are added at those frequencies where new passivity violations would otherwise have occurred.

4. Challenges with samples method

The iterative procedure in Fig. 3 is robust but it becomes computationally expensive in the case of models where several eigenvalues have passivity violations within the same violation band. To see this, consider an example with three violating eigenvalues in the same violation band, see Fig. 4, left panel. The passivity assessment will in this case pass an array $\mathbf{s2}$ containing three frequency samples. Because all three eigenvalues have a violation at all three frequencies, the passivity enforcement routine will use nine constraints as shown in the right panel. This leads to nine rows in the constraint equation. It follows that the number of constraints can become very high in the case of models with many terminals n .

The situation becomes even worse when the inner-loop feature is used. Assume that the first passivity enforcement step does not remove all violations. The subsequent (inner-loop) passivity assessment will identify the new violation extrema which are placed in array $\mathbf{s3}$ and passed to the passivity enforcement routine. Because the frequencies in $\mathbf{s3}$ do not give violations with the current model ($\{\mathbf{R}_i\}_0$), all eigenvalues of \mathbf{G} must be included in the passivity constraint equation, ensuring that the enforcement step will not bring any of these (positive) eigenvalues below the zero line. It follows that each frequency sample in $\mathbf{s3}$ results in n constraints, again contributing to the number of rows in the constraint equation. This is illustrated in Fig. 5 for a case with $n = 3$ eigenvalues where the removal of a single violation causes one new violation to arise. This results in a total of four constraints in the subsequent passivity enforcement step. Further inner-loop iterations normally lead to additional constraints.

5. Eigenpairs method

5.1. Eigenpairs

The following proposes an alternative method to the Samples method is Section 3 which differs mainly in the information passed to passivity enforcement step.

The actual building of \mathbf{C} in (5) involves the first order linearization (6) between a perturbation of \mathbf{G} and the change to its eigenvalues. It

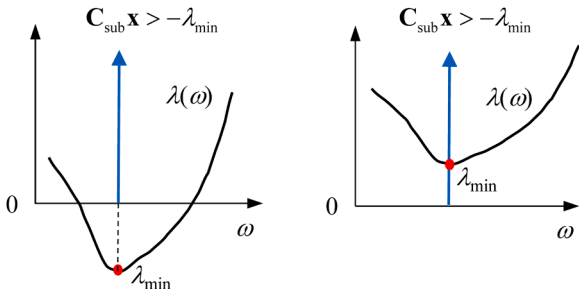


Fig. 2. Perturbation range for eigenvalue associated with frequency in $\mathbf{s2}$ (left) and $\mathbf{s3}$ (right).

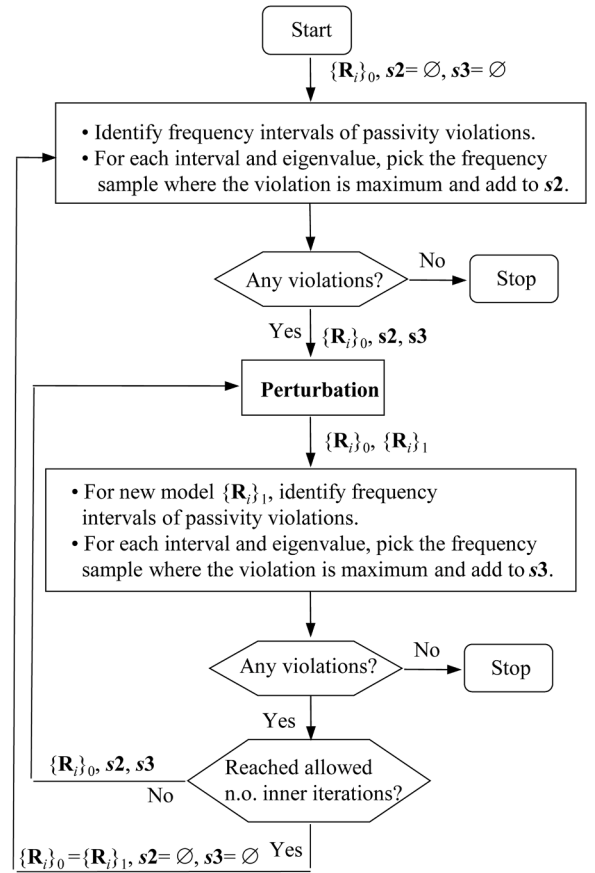


Fig. 3. Passivity assessment and enforcement by Samples method.

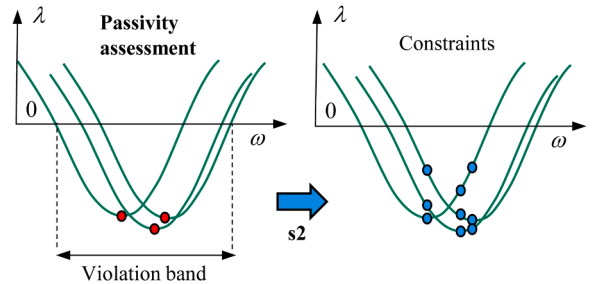


Fig. 4. Outer-loop passivity enforcement. Example with three violating eigenvalues in the same violation band. Left: Violation extrema; Right: violations used in constraint equation.

follows that the essential information needed by the passivity enforcement step are the violating eigenvalues λ_j and associated eigenvectors \mathbf{t}_j .

A new iterative scheme is therefore proposed where violating eigenpairs $(\lambda_i, \mathbf{t}_i)$ (and associated frequency points) are passed to the passivity enforcement step, instead of frequency samples alone. These eigenpairs (and frequencies) are sufficient information for building the constraint equation. The procedure is shown in Fig. 6. Consider now that one moves into the inner loop and a (new) passivity violation extremum occurs at some frequency point. For the new model $\{\mathbf{R}_i\}_1$ and considered frequency s_1 , the eigenvector of the violating eigenpair is compared against all eigenvectors of the original model $\{\mathbf{R}_i\}_0$ at s_1 , and the closest eigenvector (from original model) is identified. That eigenvector and associated eigenvalue represents the (additional) eigenpair that is to be included as constraint.

Fig. 7 shows the use of the Eigenpairs method for the illustrative example in Fig. 4 (Samples method). Only the violating eigenvalues

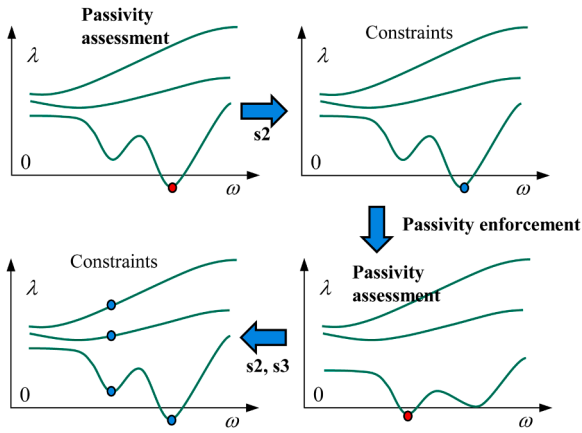


Fig. 5. Outer-loop iteration followed by one inner-loop iteration. Example with single violating eigenvalue. The single constraint used in the (outer-loop) passivity enforcement leads to four constraints in the inner-loop passivity enforcement.

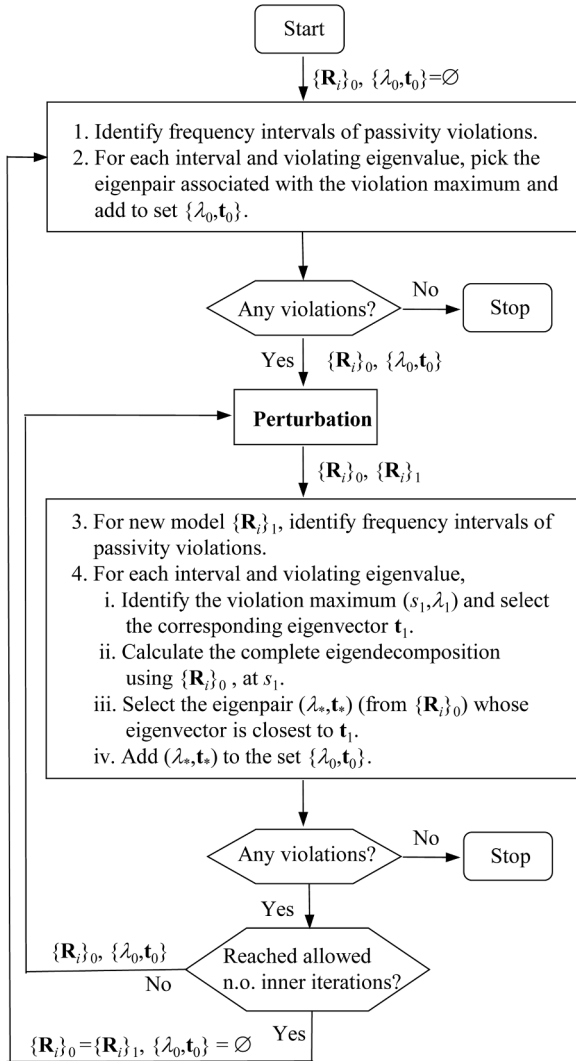


Fig. 6. Passivity assessment and enforcement by Eigenpairs method.

detected by the passivity assessment step are now used in the passivity enforcement step, reducing the number of constraints from nine to three.

Fig. 8 further shows the example with one inner-loop iteration,

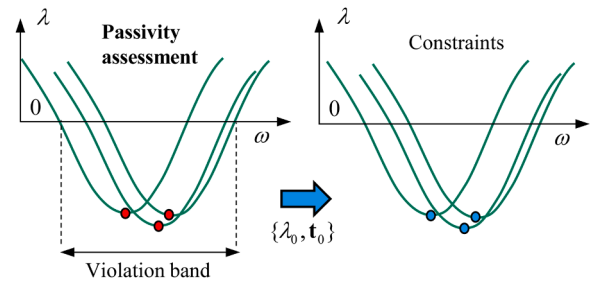


Fig. 7. Example with three violating eigenvalues in the same violation band. Left: Violation extrema; Right: Violations used in constraint equation.

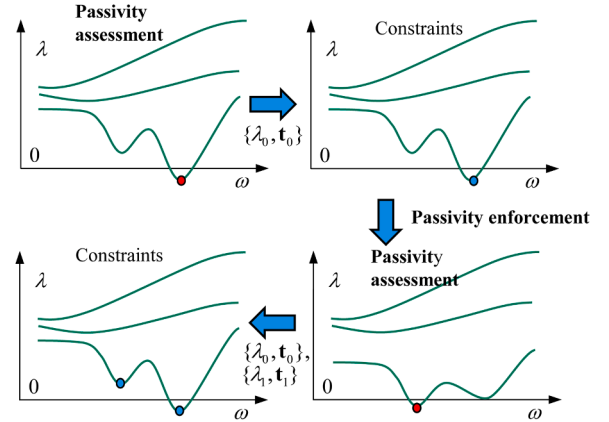


Fig. 8. Outer-loop iteration followed by one inner-loop iteration. Example with single violating eigenvalue. The single constraint used in the (outer-loop) passivity enforcement leads to two constraints in the inner-loop passivity enforcement.

corresponding to Fig. 5 in the Samples method. Only the violating eigenvalues from the outer-loop and the prospective violations from the inner-loop are now used in the passivity enforcement, reducing the number of constraints from four to two.

5.2. Including local violations

The outer-loop of the presented procedure in Fig. 7 places a single constraint at the global minimum (maximum violation) of each violating eigenvalue within a violating frequency band. The implementation also permits to include all local minima in the constraints, often reducing the number of iterations but at the cost of more constraints. All the presented examples includes local violations as constraints.

5.3. Eigenvector closeness

The selection of the closest eigenvector in step 4.iii in Fig. 6 is as follows. Consider one eigenvector t_1 obtained from the model with residue matrices $\{R_i\}_1$ and the eigenvector matrix T_0 obtained from the model with residue matrices $\{R_i\}_0$, at the same frequency. The closest eigenvector from T_0 is the one that gives the largest dot product with t_1 . That eigenvector is identified as the largest element of h in (7), where superscript H denotes transpose and conjugate.

$$h = t_1^H T_0 \quad (7)$$

5.4. Eigenvector tracking

With both the Samples method and Eigenpairs method it is necessary to identify passivity violation maxima using a frequency sweep. When performing a frequency sweep, the eigenvalue calculation routine may

interchange the sequence of eigenvalues when moving from one frequency point to the next. Such switchovers lead to abrupt changes in plots of eigenvectors and spurious maxima and minima of the eigenvalues. The occurrence of such artificial switchovers is removed by usage of an eigenvector tracking procedure [26] which assesses dot products between the eigenvectors belonging to two successive frequency samples k and $k+1$. The product \mathbf{h}_j between the j th eigenvector $\mathbf{t}_{k+1,j}^H$ and all eigenvectors of \mathbf{T}_k is calculated. The index l to the largest element of \mathbf{h}_j defines the corresponding eigenvector $\mathbf{t}_{k,l}$ of \mathbf{T}_k . By looping through the eigenvectors $\mathbf{t}_{k+1,j}^H$, $j = 1, \dots, n$, a new column sequence for \mathbf{T}_{k+1} is established, see Algorithm 1.

Additional robustness is achieved by making the interchanging in a prioritized sequence such that $\max(h_j)$ appears in descending sequence in the loop of Algorithm 1. The procedure gives excellent results provided that the frequency step length is sufficiently small.

6. Solving using RP-NNLS

The constrained LS problem (5) was in the original RP implementation [13] solved using a quadratic programming method. It was later shown [24] that the computational efficiency can be greatly improved by transforming (5) into a least distance problem via QR factorization and solved as a non-negative least squares (NNLS) problem [27], leading to the RP-NNLS method. We recall here the main steps of the procedure, referring to [24] for the details.

Matrix \mathbf{A} in (5) is subjected to QR factorization, giving

$$\min_{\mathbf{x}} \|\overline{\mathbf{Q}}\mathbf{R}\mathbf{x}\| \quad s.t. \quad \mathbf{C}\mathbf{x} > \mathbf{d} \quad (8)$$

Pre-multiplying with $\overline{\mathbf{Q}}^T$ and introducing the change of variable $\mathbf{y} = \overline{\mathbf{R}}\mathbf{x}$ leads to a least distance problem,

$$\min_{\mathbf{y}} \|\mathbf{y}\| \quad s.t. \quad \overline{\mathbf{C}}\mathbf{R}^{-1}\mathbf{y} > \mathbf{d} \quad (9)$$

Introducing matrices \mathbf{E} and \mathbf{f} in (10) permits the problem (9) to be solved as the NNLS problem (11). Vectors \mathbf{y} and \mathbf{x} are recovered by (12) and (13) using the solution residual (14). In (12), col_E is the number of columns of \mathbf{E} .

$$\mathbf{E} = \begin{bmatrix} (\overline{\mathbf{C}}\mathbf{R}^{-1})^T \\ \mathbf{d}^T \end{bmatrix}, \quad \mathbf{f} = [0, \dots, 0, 1]^T \quad (10)$$

$$\min_{\mathbf{u}} \|\mathbf{E}\mathbf{u} - \mathbf{f}\| \quad s.t. \quad \mathbf{u} \geq \mathbf{0} \quad (11)$$

$$\mathbf{y} = \frac{\boldsymbol{\varepsilon}(1 : \text{col}_E - 1)}{\boldsymbol{\varepsilon}(\text{col}_E)} \quad (12)$$

$$\mathbf{x} = \overline{\mathbf{R}}^{-1}\mathbf{y} \quad (13)$$

$$\boldsymbol{\varepsilon} = \mathbf{f} - \mathbf{E}\mathbf{u} \quad (14)$$

The solving of (11) is usually very fast since \mathbf{E} has few columns. The dimension of \mathbf{E} is $n^2(N+1) \times (L+1)$ where L is the number of constraints (rows in \mathbf{C}). The QR factorization (8) is applied independently to the individual blocks of the block-diagonal \mathbf{A} , thereby giving a very fast factorization [24]. The block-feature is also utilized in (13) where the inversion of $\overline{\mathbf{R}}$ is achieved via independent inversion of its small sub-blocks [24].

7. Example: transformer branch impedance modeling

This example demonstrates the computational advantages of the proposed Eigenpairs method (Section 5) over the existing Samples method (Section 3).

7.1. Branch impedance matrix

We return to the example in [24] of white-box transformer frequency-dependent branch impedance modeling. The considered transformer is a 1-pH 50 MVA three-winding transformer with rated voltage 230/69/13.8 kV. The branch impedance matrix \mathbf{Z}_b has dimension 213×213 and was fitted using vector fitting (VF) between 60 Hz and 1.08 MHz using a 10th order pole-residue model, including \mathbf{R}_0 . Fig. 9 shows the eigenvalues of $\mathbf{G}(\omega)$. It is observed that several passivity violations exist at high frequencies as well as one violation at low frequencies.

Passivity is to be enforced using either the Eigenpairs method or the Samples method. With both methods, the actual solving is done using RP-NNLS. The LS part of (5) is established at the same $K = 14$ frequency samples used in VF for extracting the non-passive model. Inverse LS weighting is used of the individual matrix elements (i, j),

$$\text{weight}_{i,j}(\omega) = \frac{1}{\sqrt{Z_b(i,j)(\omega)}} \quad (15)$$

7.2. Passivity enforcement using outer-loop iterations

It is first assumed that the inner-loop feature is not used. With both methods, each band with passivity violations is scanned using $N_{int} = 21$ linearly spaced samples. Fig. 10 shows a zoomed view of the band with high-frequency violations. The figure includes the points used as constraints by the two strategies. Due to the coarse resolution (21 samples), the Eigenpairs method places the violations at three distinct frequencies, with a single violation per eigenvalue. With the Samples method, the violations are placed at the same frequencies, but with three violations per eigenvalue. This result is compliant with the illustrative example in Figs. 4 and 7.

With the Samples method, the situation deteriorates as the resolution of the passivity scan (in each violation band) increases. Fig. 11 shows the same result as in Fig. 8 when scanning using $N_{int} = 201$ samples per violation band. The number of constraint points now increases strongly with the Samples method while it remains unchanged with the Eigenpairs method.

In the actual implementation, the scan is done using a combination of logarithmically spaced samples and linearly spaced samples, thereby also capturing smooth eigenvalue behaviors at low frequencies.

With $N_{int} = 42$ combined samples, the resulting \mathbf{E} -matrix gets with the Samples method 227,911 rows and 151 columns in the first iteration while the number of columns is 39 with the Eigenpairs method. The impact on the computational performance is shown in Table 1, including all iterations. It is seen that the resulting perturbation error is about the same with both methods. But the Eigenpairs method leads to a shorter computation time (7.9 s. vs 18.4 s). The reduction is due to faster

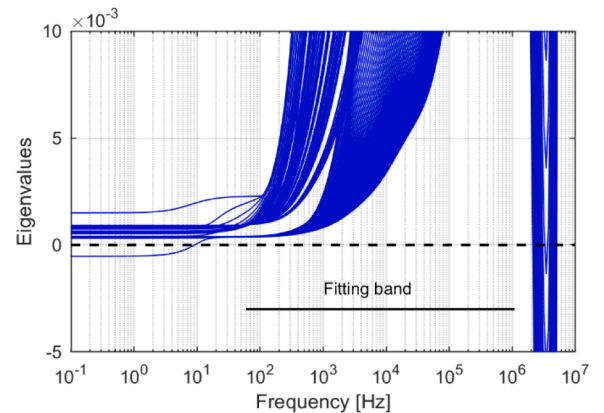


Fig. 9. Passivity violations.

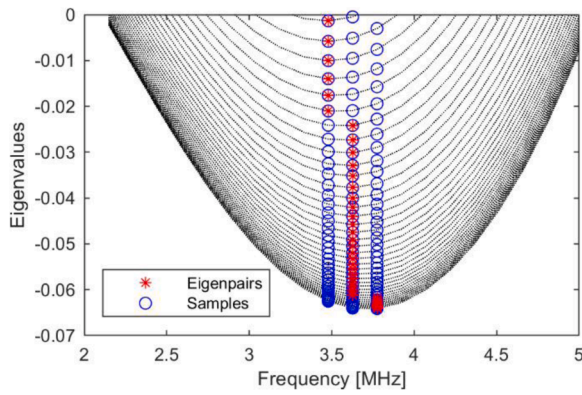


Fig. 10. High-frequency violations and selected constraints (first iteration). Resolving violation band using 21 samples.

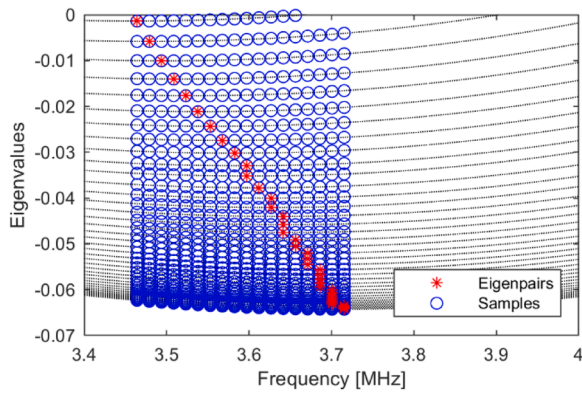


Fig. 11. High-frequency violations and selected constraints (first iteration). Resolving violation band using 201 samples.

Table 1
Outer loop iterations. computational metrics. $N_{int} = 42$ samples.

Method	Iterations	Solve NNLS [sec]	Total [sec]	Rmserr (weighted)
Eigenpairs	6	2.2	7.9	5.1×10^{-5}
Samples	5	8.9	18.4	5.0×10^{-5}

building of the constraint matrix and faster solving of the NNLS problem. The relative difference between the two methods is even higher with $N_{int} = 402$, see Table 2. The number of columns with the two approaches is now respectively 946 and 40 in the first iteration. The computational performance in Table 2 shows that the Eigenpairs method gives about five times faster calculation. It is observed that with the Samples method, slightly fewer iterations are needed. This result is as expected since the additional constraints reduce the probability that new violations will appear at the associated frequencies.

7.3. Passivity enforcement including one inner loop iteration

It was shown in Sections 4 and 5 that with usage of the inner-loop iteration, the Samples method leads to many new constraints while the increase in constraints is moderate with the Eigenpairs method. To

Table 2
Outer loop iterations. Computational metrics. $N_{int} = 402$ samples.

Method	Iterations	Solve NNLS [sec]	Total [sec]	Rmserr (weighted)
Eigenpairs	7	2.3	11.5	5.1×10^{-5}
Samples	5	27.2	49.0	4.9×10^{-5}

demonstrate this, consider again the example with scanning of each violation band using 21 logarithmically and 21 linearly spaced frequency samples. Table 3 shows the result with a single inner-loop iteration, using either the Eigenpairs method or the Samples method. Comparison with Table 1 (no inner-loop iteration) shows that the calculation time by the Eigenpairs method increases from 7.9 s to 13.8 s while the calculation did not finish with the Samples method. It was observed that in the first inner-loop iteration, the number of columns in E with the two methods was 76 and 1855, respectively.

8. Example: grounding mat modeling

Passivity enforcement should normally be applied only for cases with small violations within the considered frequency band since the removal of large violations can entirely corrupt the model's behavior. To properly test the new passivity enforcement routine we will still apply it to one case where there exist substantial in-band passivity violations.

The example is a grounding mat of size 100×100 m with 10 m mesh size. The mesh is buried one meter below the surface of a soil with resistivity $1000 \Omega\cdot\text{m}$ and relative permittivity $\epsilon_r = 3$. The frequency-dependent admittance matrix Y with respect to the $n = 121$ corner points was calculated at 150 frequency samples between 10 Hz and 10 MHz using a numerical method [29,30]. The admittance matrix has been fitted by a pole-residue model with $N = 30$ poles.

Fig. 12 shows the eigenvalues of G, before and after passivity enforcement using the Eigenpairs method while Fig. 13 compares the admittance elements of the original model with those of the perturbed model. The calculation made use of the inverse weighting (15) and outer-iterations only. Table 4 shows the calculation performance. The passivity is enforced in 75.2 s in 8 iterations, with 508 constraints in the first iteration. Table 4 also includes the result when using fewer free variables via the residue matrix bandwidth, defined by parameter bw [24]. (Choosing $bw=120$ uses all elements while $bw=0$ uses only diagonal elements). It is observed that the calculation time is strongly reduced with reduced bw , although the (weighted) rms-error increases. Also, the required number of iterations increases. For comparison, usage of the Samples method required a total of 127.8 s, 35.6 s and 6.9 s, with $bw = 0, 10$ and 120, respectively.

9. Example: Wide-band transformer modeling

In the case of small-scale problems, the RP-NNLS is very fast also with many inactive constraints and the Eigenpairs method will not offer significant advantage over the Samples method. As example we consider the passivity enforcement of a measurement-based model of a HVDC transformer. The model obtained via VF has $n = 5$ terminals and $N = 90$ poles. Details of the transformer and the model extraction using VF are given in [31].

Fig. 14 shows the result from passivity enforcement by RP-NNLS with usage of the Eigenpairs method and the test matrix (3) for passivity assessment, with two inner-loop iterations. It is observed that all negative eigenvalues of $G(\omega)$ have been removed, i.e. the model has become passive. The passivity enforcement made use of inverse magnitude weighting of the individual elements of $Y(\omega)$ and two inner-loop iterations.

Table 5 shows the calculation time and the resulting (weighted) rms error of the passivity enforcement. The result is compared with that

Table 3
Outer loop iterations in combination with one inner-loop iteration. $N_{int} = 42$ samples.

Method	Outer-loop iterations	Solve NNLS [sec]	Total [sec]	Rmserr (weighted)
Eigenpairs	4	5.8	13.8	4.8×10^{-5}
Samples	–	–	–	–

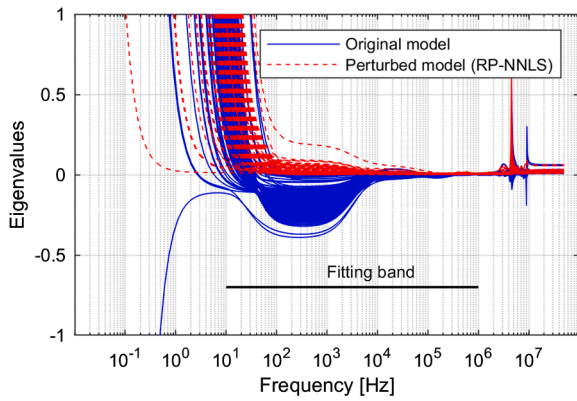


Fig. 12. Passivity enforcement using Eigenpairs method. Impact on eigenvalues of $G(\omega)$.

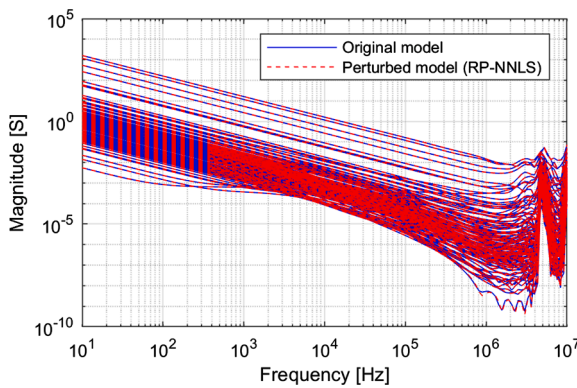


Fig. 13. Passivity enforcement using Eigenpairs method. Impact on elements of $Y(\omega)$.

Table 4
Outer loop iterations using eigenpairs method. $N_{int} = 21$ samples.

bw	Iterations	Solve NNLS [sec]	Total [sec]	Rmserr (weighted)
120	8	48.7	64.1	0.0039
10	18	10.2	16.5	0.0062
0	16	0.71	2.6	0.0093

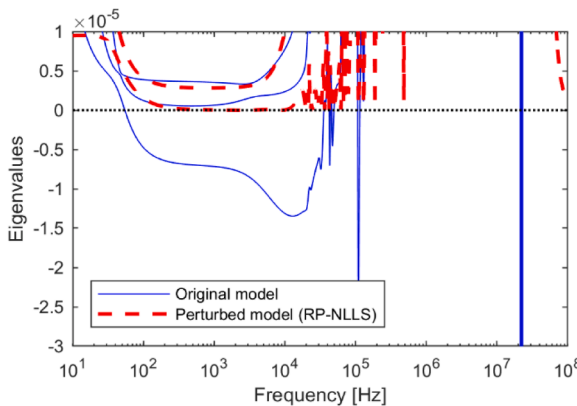


Fig. 14. Passivity enforcement using Eigenpairs Method. Impact on elements of $G(\omega)$.

Table 5
Outer loop iterations in combination with two inner-loop iterations.

Method	Outer-loop iterations	Solve NNLS [sec]	Total [sec]	Rmserr (weighted)
Eigenpairs	4	0.10	0.53	0.0135
Samples	4	0.14	0.78	0.0136

obtained with usage of the Samples method. The two methods are seen to produce a model with practically the same error, but the Eigenpairs method is 0.25 s (47%) faster. The passivity assessment did however require about 1.5 s so that the two methods are in practice equal.

The reason for the faster computation by usage of the Eigenpairs method can again be attributed to the lower number of constraints, i.e. columns of E in (11). Tables 6 and 7 compare number of constraints in each iteration, using either the Eigenpairs method or the Samples method. It is seen that the Eigenpairs method results in fewer constraints than the Samples method, thereby permitting faster building of the constraint matrix and faster solving of the NNLS problem as well.

10. Discussion

10.1. Computational advantages of eigenpairs method over samples method

The use of the Eigenpairs method over the Samples method was shown to result in a substantial reduction in computation time for the passivity enforcement when the model was large. This time reduction is a consequence of the lower number of considered violations with the Eigenpairs method. The constraint equation in (5) therefore gets fewer rows, which implies faster building of matrix C in (5). (It is shown in [24] that the cost of building C is substantial). Second, the solving of (11) becomes faster since the lower number of rows in C implies fewer columns in E in (10). The lower number of columns in E reduces the calculation time for solving (11) by the active set method, in part because fewer internal iterations are needed. Another advantage is lower memory requirements since E is the largest matrix to be stored with RP-NNLS.

10.2. Passivity assessment

The presented CPU times in the Tables are for the passivity enforcement alone. With large scale problems such as the presented examples in Sections 7 and 8, the passivity assessment can only be achieved using eigenvalue sweeping over a set of discrete frequencies. In the branch impedance example, the initial sweeping for detecting violation bands was performed using 301 samples, followed by a fine sweep using 42 samples per violating band for detection of violation extrema values. The passivity assessment required a total of 7.5 s, compared to the 7.9 s for the passivity enforcement (Table 1). In the ground mat example, the initial sweeping was performed using 202 samples and a total 10.2 s was used for passivity assessment, compared to 75.2 s for the passivity enforcement with $bw=120$. Increasing the sampling density will necessarily increase the total time for passivity assessment.

Table 6
Eigenpairs method. Number of constraints in each iteration.

	iter_out=1	iter_out=2	iter_out=3	iter_out=4
iter_in=0	16	23	24	5
iter_in=1	33	44	29	–
iter_in=2	52	60	34	–

Table 7
Samples method. Number of constraints in each iteration.

	iter_out=1	iter_out=2	iter_out=3	iter_out=4
iter_in=0	33	27	22	4
iter_in=1	138	181	71	–
iter_in=2	293	286	111	–

Algorithm 1

```

 $\hat{\mathbf{T}}_{k+1} = \mathbf{T}_{k+1}$ 
for  $j = 1:n$ 
  Calculate  $\mathbf{h}_j = \mathbf{t}_{k+1,j}^H \mathbf{T}_k$ 
  Calculate index  $l(j)$  to  $\max(\mathbf{h}_j)$ 
  Set  $\mathbf{T}_k(:,l(j)) = \mathbf{0}$ 
end
 $\mathbf{T}_{k+1} = \hat{\mathbf{T}}_{k+1}(:,l)$ 

```

10.3. Alternative passivity enforcement method

An alternative passivity enforcement scheme is the one included in the freely available Matrix Fitting Toolbox mentioned in Section 3. That scheme makes use of the Samples method in combination with residue eigenvalue perturbation [14]. In the case of the transformer example in Section 9, passivity was enforced in 35 s (excluding passivity assessment), compared to 0.53 s with the approach presented in this work (Table 5). In the case of the branch impedance and grounding mat examples (Sections 7 and 8), the passivity enforcement by Matrix Fitting Toolbox failed because of excessive memory requirements.

10.4. Passivity violations

With usage of vector fitting (VF), the occurrence of passivity violations in the model is dependent on the selection of frequency samples, the specified model order, and the adopted LS weighting scheme. In general, the use of an excessive model order tends to increase the number and severity of passivity violations. Also, the use of inverse least squares weighting schemes in VF tends to produce more passivity violations. Typically, the most severe violations occur at out-of-band frequencies, for instance as observed in Fig. 12. Severe violations can also occur between the support frequency samples that were used to obtain the model using vector fitting. A good practice is to choose the frequency samples such that the model behavior is well resolved, and then choose a model order which captures the essential behavior of the frequency responses.

11. Conclusion

A new iterative passivity assessment and enforcement scheme has been presented for use with the residue perturbation (RP) method. The passivity assessment routine identifies local passivity violations and passes the associated eigenpairs to the passivity enforcement routine. This approach gives substantial savings in computation time for the RP solver known as RP-NNLS, compared to an earlier scheme where only frequency samples with passivity violations are passed to RP-NNLS. The new scheme permits to enforce passivity of models with a high number of terminals with acceptable CPU times.

Credit author statement

- 1 Conception or design of the work: Bjørn Gustavsen
- 2 Data collection.: Bjørn Gustavsen
- 3 Data analysis and interpretation.: Bjørn Gustavsen
- 4 Drafting the article.: Bjørn Gustavsen
- 5 Critical revision of the article.: Bjørn Gustavsen

6 Final approval of the version to be published.: Bjørn Gustavsen

Declaration of Competing Interest

I wish to confirm that there are no known conflicts of interest associated with this publication and there has been no significant financial support for this work that could have influenced its outcome. I confirm that the manuscript has been read and approved by all named authors (I am sole author) and that there are no other persons who satisfied the criteria for authorship but are not listed.

I confirm that I have given due consideration to the protection of intellectual property associated with this work and that there are no impediments to publication, including the timing of publication, with respect to intellectual property. In so doing I confirm that I have followed the regulations of our institutions concerning intellectual property.

Acknowledgement

The author thanks Dr. Andrzej Holdyk (SINTEF Energy Research, Trondheim, Norway) for providing the grounding mat data set in Section 9.

References

- [1] J.R. Marti, Accurate modelling of frequency-dependent transmission lines in electromagnetic transient simulations, *IEEE Trans. Power Appar. Syst. PAS-101* (1) (Jan. 1982) 147–157.
- [2] E.S. Banuelos-Cabral, B. Gustavsen, J.A. Gutierrez-Robles, H.K. Høidalen, J. L. Naredo, Computational efficiency improvement of the universal line model by use of rational approximations with real poles, *Electric Power Syst. Res.* 140 (2016) 424–434.
- [3] S. Morched, J.H. Ottevangers, L. Marti, Multi-port frequency dependent network equivalents for the EMTP, *IEEE Trans. Power Del.* 8 (3) (July 1993) 1402–1412.
- [4] U.D. Annakkage, et al., Dynamic System Equivalents: a survey of available techniques, *IEEE Trans. Power Del.* 27 (1) (Jan. 2012) 411–420.
- [5] D.N. Hussein, M. Matar, R. Irvani, A wideband equivalent model of type-3 wind power plants for EMT studies, *IEEE Trans. Power Del.* 31 (5) (Oct. 2016) 2322–2331.
- [6] Ramirez, et al., Application of balanced realizations for model-order reduction of dynamic power system equivalents, *IEEE Trans. Power Del.* 31 (5) (Oct. 2016) 2304–2312.
- [7] D. Filipović-Grčić, B. Filipović-Grčić, I. Uglešić, High-frequency model of the power transformer based on frequency-response measurements, *IEEE Trans. Power Del.* 30 (1) (Feb. 2015) 34–42.
- [8] B. Gustavsen, Á. Portillo, R. Ronchi, A. Mjelve, High-frequency resonant overvoltages in transformer regulating winding caused by ground fault initiation on feeding cable, *IEEE Trans. Power Del.* 33 (2) (April 2018) 699–708.
- [9] B. Gustavsen, A. Semlyen, Rational approximation of frequency domain responses by vector fitting, *IEEE Trans. Power Del.* 14 (3) (July 1999) 1052–1061.
- [10] S. Lefteriu, A.C. Antoulas, A new approach to modeling multiport systems from frequency-domain data, *IEEE Trans. Comput.-Aided Des. Integrat. Circuit. Syst.* 29 (1) (Jan. 2010) 14–27.
- [11] J. Morales Rodriguez, E. Medina, J. Mahseredjian, A. Ramirez, K. Sheshyekani, I. Kocar, Frequency-domain fitting techniques: a review, *IEEE Trans. Power Del.* 35 (3) (June 2020) 1102–1110.
- [12] P. Triverio, S. Grivet-Talocia, M. Nakhla, F.G. Canavero, R. Achar, Stability, causality and passivity in interconnect models, *IEEE Trans. Adv. Packag.* 30 (4) (2007) 795–808.
- [13] B. Gustavsen, A. Semlyen, Enforcing passivity for admittance matrices approximated by rational functions, *IEEE Trans. Power Syst.* 16 (Feb. 2001) 97–104.
- [14] B. Gustavsen, Fast passivity enforcement for pole-residue models by perturbation of residue matrix eigenvalues, *IEEE Trans. Power Del.* 23 (4) (October 2008) 2278–2285.
- [15] S. Grivet-Talocia, Passivity enforcement via perturbation of Hamiltonian matrices, *IEEE Trans. Circuits Syst.* 51 (9) (Sept. 2004) 1755–1769.
- [16] D. Saraswat, R. Achar, M.S. Nakhla, Global passivity enforcement algorithm for macromodels of interconnect subnetworks characterized by tabulated data, *IEEE Trans. Very Large Scale (VLSI) Syst.* 13 (7) (July 2005) 819–832.
- [17] S. Grivet-Talocia, A. Ubolli, A comparative study of passivity enforcement schemes for linear lumped macromodels, *IEEE Trans. Adv. Packag.* 31 (4) (Nov. 2008) 673–683.
- [18] E. Medina, A. Ramirez, J. Morales, K. Sheshyekani, Passivity enforcement of FDNEs via perturbation of singularity test matrix, *IEEE Trans. Power Del.* 35 (4) (August 2020) 1648–1655.
- [19] S. Boyd, L.O. Chua, On the passivity criterion for LTI n-ports, *Circuit Theory Appl.* 10 (1982) 323–333.
- [20] Semlyen, B. Gustavsen, A half-size test matrix for fast and reliable assessment of rational models, *IEEE Trans. Power Del.* 24 (1) (Jan. 2009) 345–351.

- [21] P. Coelho, J. Phillips, L.M. Silveira, A convex programming approach for generating guaranteed passive approximations to tabulated frequency-data, *IEEE Trans. Comput.-Aided Des. Integrat. Circuit. Syst.* 23 (2) (Feb. 2004) 293–301.
- [22] L.P.R K. Ihlenfeld, G.H.C. Oliveira, On the optimality of passive and symmetric high-frequency n-terminal transformer models, *IEEE Trans. Power Del.* 34 (1) (Feb. 2019) 129–136.
- [23] S. Grivet-Talocia, B. Gustavsen, *Passive Macromodeling: Theory and Applications*, John Wiley and Sons, 2015.
- [24] B. Gustavsen, "Passivity enforcement by residue perturbation via constrained non-negative least squares", *IEEE Trans. Power Del.*, doi: 10.1109/TPWRD.2020.3026385. Online <https://ieeexplore.ieee.org>.
- [25] B. Gustavsen, Computer code for passivity enforcement of rational macromodels by residue perturbation, *IEEE Trans. Adv. Packag.* 30 (2) (May 2007) 209–215.
- [26] L.M. Wedepohl, H.V. Nguyen, G.D. Irwin, Frequency-dependent transformation matrices for untransposed transmission lines using Newton-Raphson method, *IEEE Trans. Power Syst.* 11 (3) (Aug. 1996) 1538–1546.
- [27] C.L. Lawson, R.J. Hanson, *Solving Least Squares Problems*, SIAM, 1995. ISBN 0-89871-356-0.
- [28] G.H. Golub, C.V. Van Loan, *Matrix Computations*, The John Hopkins University Press, 1989. ISBN 08018-3739-1.
- [29] C.S. Lima, R.A.R. Moura, P.H.N. Vieira, M.A.O. Schroeder and M.T. Correia de Barros, "A computational improvement in grounding systems transient analysis," *IEEE Trans. Electromagnetic Compatibility*, vol. 62, no. 3, pp. 765–773.
- [30] S. Visacro, A. Soares, HEM: a model for simulation of lightning-related engineering problems, *IEEE Trans. Power Del.* 20 (2) (April 2005) 1206–1208.
- [31] B. Gustavsen, Y. Vernay, Measurement-based frequency-dependent model of a HVDC transformer for electromagnetic transient studies, *Electric Power Syst. Res.* (2020), 106141. EPSR 17011 pages.

Bjørn Gustavsen was born in Norway in 1965. He received the M.Sc. degree and the Dr. Ing. degree in Electrical Engineering from the Norwegian Institute of Technology (NTNU) in Trondheim, Norway, in 1989 and 1993, respectively. Since 1994 he has been working at SINTEF Energy Research where he is currently a Chief Research Scientist. He is also an adjunct Professor at NTNU, since 2020. His interests include simulation of electromagnetic transients and modeling of frequency dependent effects. He spent 1996 as a Visiting Researcher at the University of Toronto, Canada, and the summer of 1998 at the Manitoba HVDC Research centre, Winnipeg, Canada. He was a Marie Curie Fellow at the University of Stuttgart, Germany, August 2001–August 2002.